Electronic Supplementary Material (ESI) for Journal of Materials Chemistry A.
This journal is © The Royal Society of Chemistry 2022

Supporting information

Bio-inspired Self-healing Flexible Films with Pomegranate-shaped Nanospheres Loaded Graphene for Electromagnetic Interference Shielding and Superhydrophobicity Performances

*Jianlin Zhou[a], Zhonghua Yuan[a], Han Liu[a], Weixing He[b], Kejing Yu[a], Kunlin Chen[a]**

a, Key Laboratory of Eco-Textile, Ministry of Education, School of Textile Science and Engineering, Jiangnan University, Wuxi 214122, China, E-mail: chenkunlin@jiangnan.edu.cn

b, Jiangsu Textile Research Institute Co. Ltd, Wuxi 214122, China

Keywords: bio-inspired, nanospheres, films, self-healing, EMI shielding

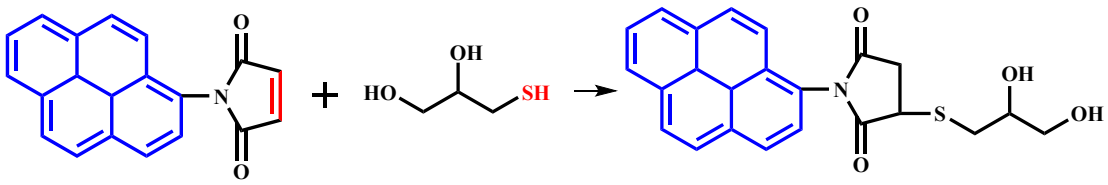

Fig. S1 The synthetic route of M-NPM

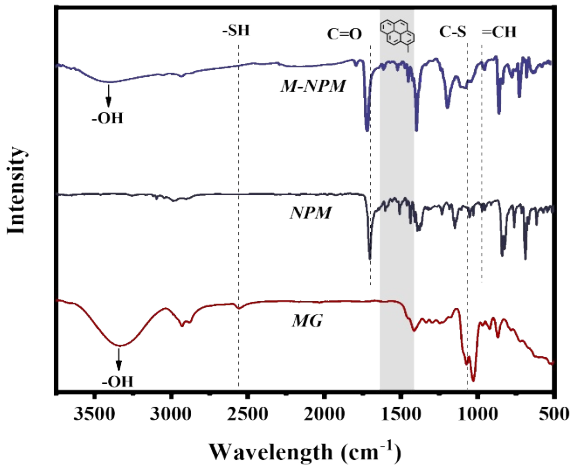

Fig. S2 FT-IR spectra of MG, NPM and M-NPM

The characteristic peaks (1600cm^{-1}, 1508cm^{-1} and 1437cm^{-1}) of pyrene structure were observed in NPM sample as well as M-NPM sample. The -OH stretching (3400 cm^{-1}) and C-S bending (1068 cm^{-1}) could be both observed in MG sample and M-NPM sample. Moreover, the absorption peak in 2560 cm^{-1} related to -SH of MG and the absorption peak in 967 cm^{-1} related to -CH=CH- of NPM were found in M-NPM, illustrating successful preparation of pyrene-containing dihydric alcohol.

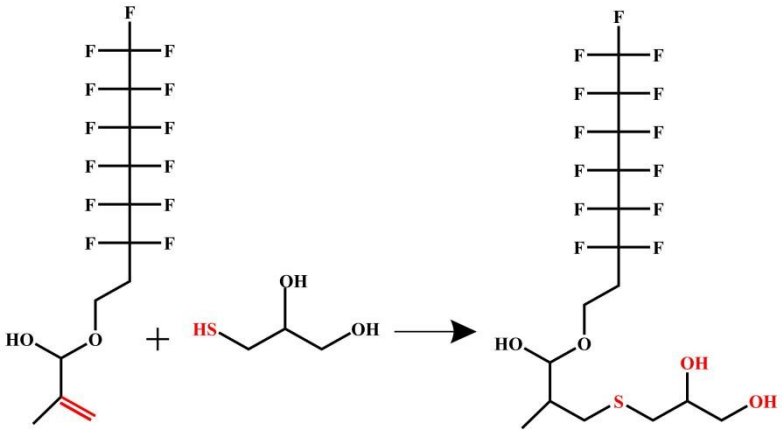

Fig. S3 The synthetic route of M-PFM

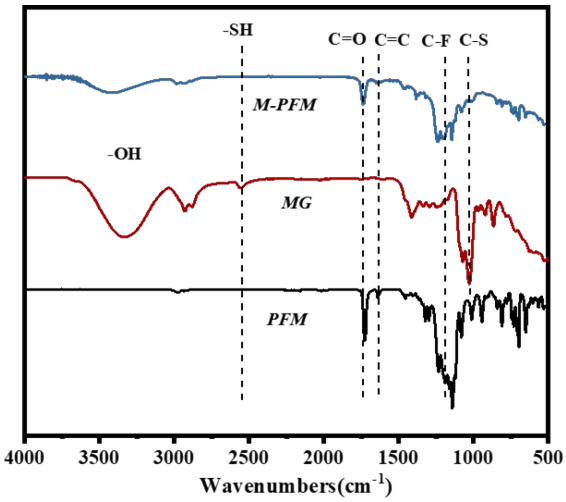

Fig. S4 FT-IR spectra of MG, PFM and M-PFM

The FT-IR spectra of PFM consisted of three characteristic absorption bands, i.e., C=O (1720 cm^{-1}), C=C (1636 cm^{-1}) and C-F (1195 cm^{-1}). For M-PFM, the absorption bands of 3400 cm^{-1} (-OH) and 1037 cm^{-1}(C-S) pertained to the monothioglycerol (MG), and the disappearance of absorption band derived to C=C clearly demonstrated that the MG successfully reacted with PFM via thiol-ene click chemistry reaction.

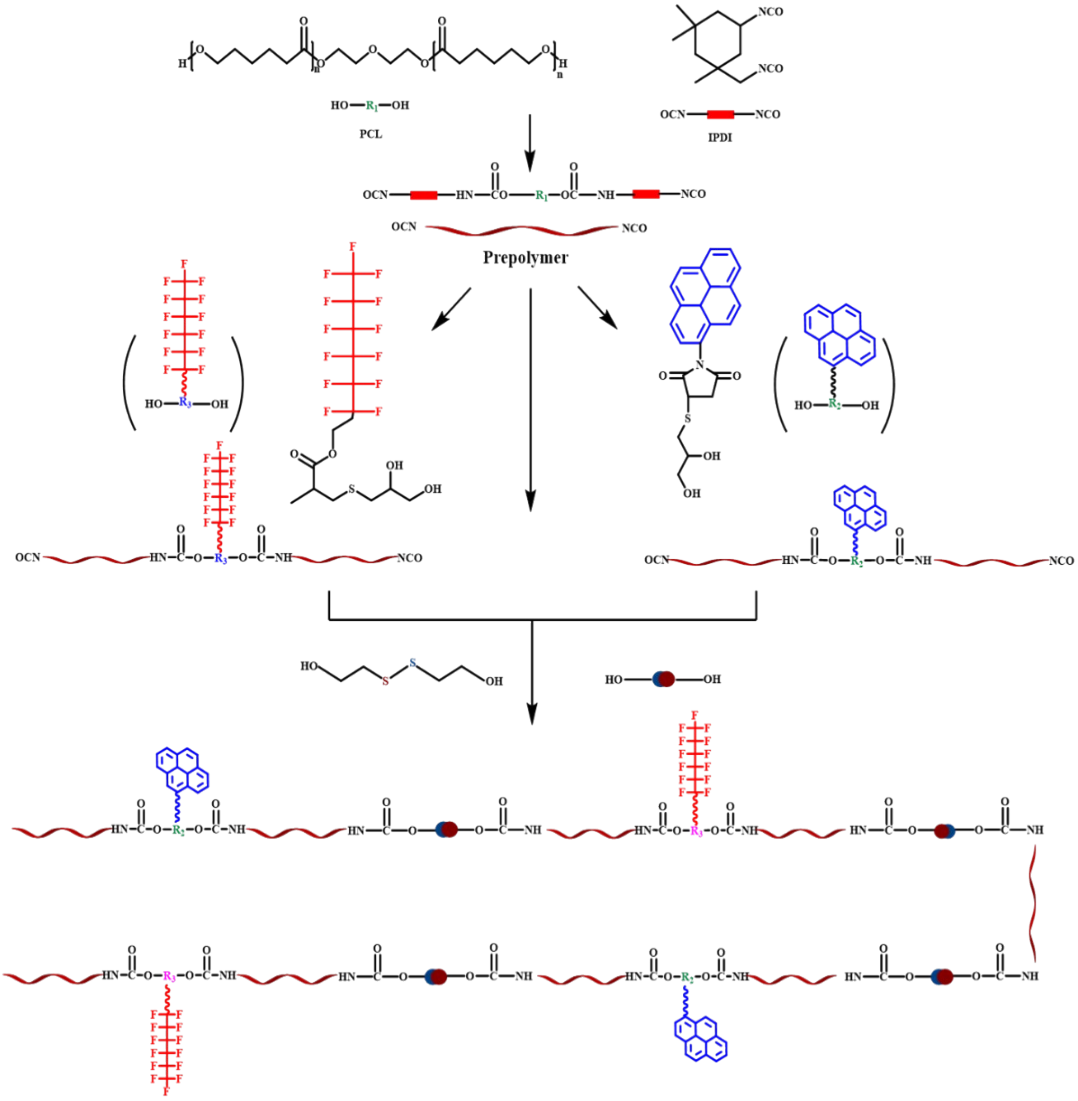

Fig. S5 The synthetic route of MPU

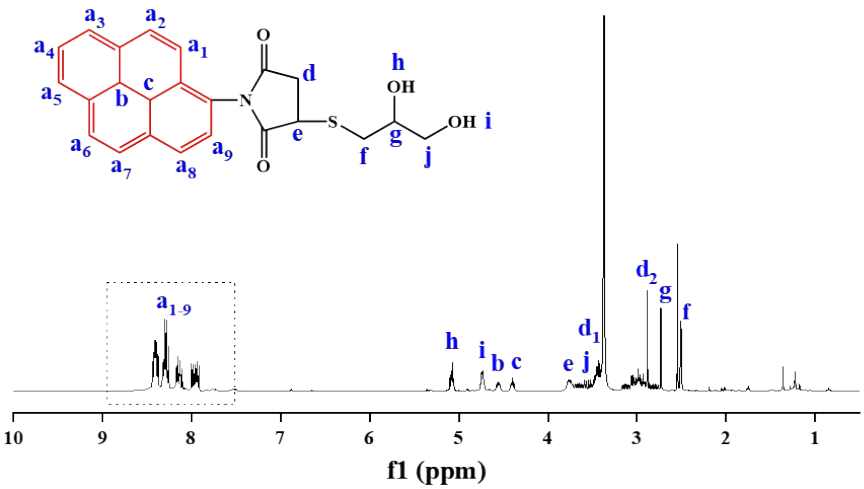

Fig. S6 ^{1}H NMR spectrum of M-NPM

The signal distribution of M-NPM is as follows: ^{1}H NMR (400 MHz, DMSO) δ 8.56 (m, 6H), 8.31 (m, 5H), 8.1 (m, 4H), 8.09 (m, 5H), 5.12 (m, 4H), 4.89 (m, 3H), 4.55 (m, 3H), 4.40 (m, 3H), 3.76 (d, J = 5.4 Hz, 3H), 3.61(m, 3H), 3.43 (s, 4H), 2.89 (s, 4H), 2.73 (s, 4H), 2.51 (s, 3H).

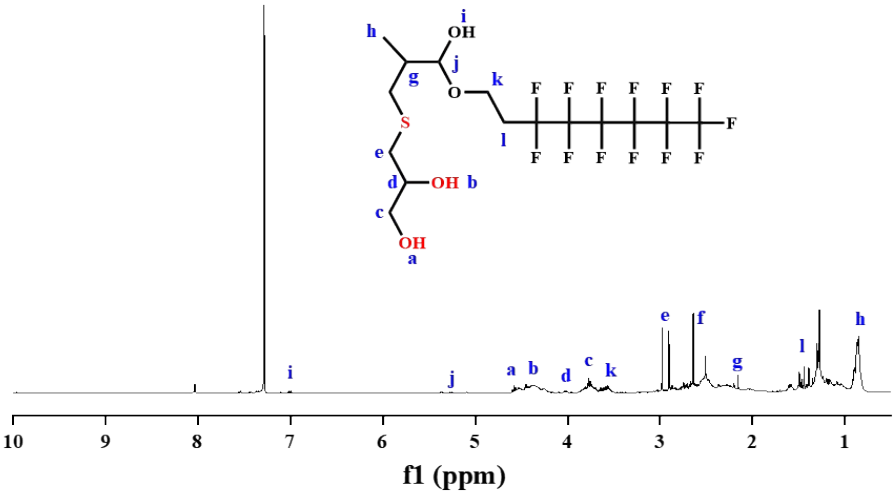

Fig. S7 ^{1}H NMR spectrum of M-PFM

The signal distribution of M-PFM is as follows: ^{1}H NMR (400 MHz, CDCl3) δ 6.71 (s, 3H), 4.58 (s, 5H), 4.44 (s, 4H), 4.02 (s, 3H), 3.78 (s, 2H), 3.57 (s, 4H), 2.98 (s, 2H), 2.64 (s, 4H), 2.16 (s, 2H), 1.28 (s, 8H), 0.85 (s, 2H).

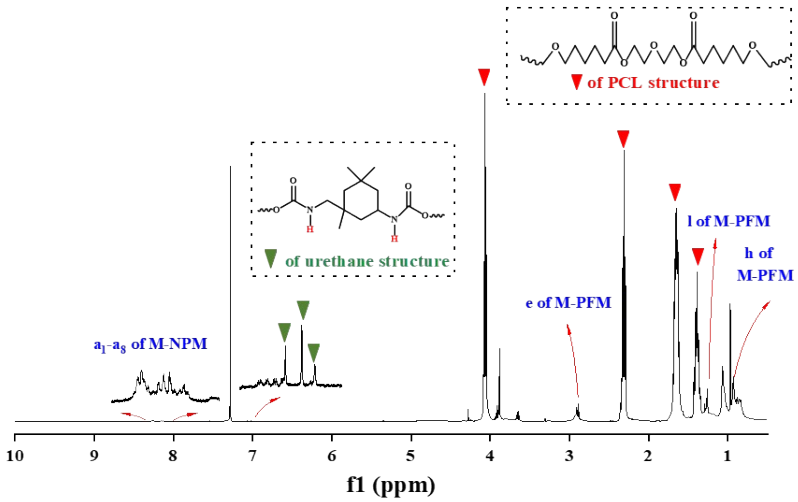

Fig. S8 ^{1}H-NMR spectrum of MPU

In the case of MPU, the signal peaks of the protons attributed to the benzene ring in the polymer can be observed at 8.42-8.05 ppm, possibly due to the graft of pyrene groups. The weak peak at 7.20-6.91 ppm is the proton peak of N–H in urethane structure. A chemical shift of 4.50-2.36 ppm is assigned to the PCL protons. Resonances in the 1.28 ppm correspond to methylene proton attached to a difluorinated group (-CH_2-CF_2 -) in the grafted M-PFM structure. The signals between 0.92 and 0.85 ppm mainly ascribe to the protons of methyl proton (CH_3-) in grafted M-PFM. As well, the peaks around 2.93-2.89 ppm are resulted from the proton of the methylene group adjacent to the thioether group. The chemical shift of protons as described above confirmed the structural characteristics of MPU.

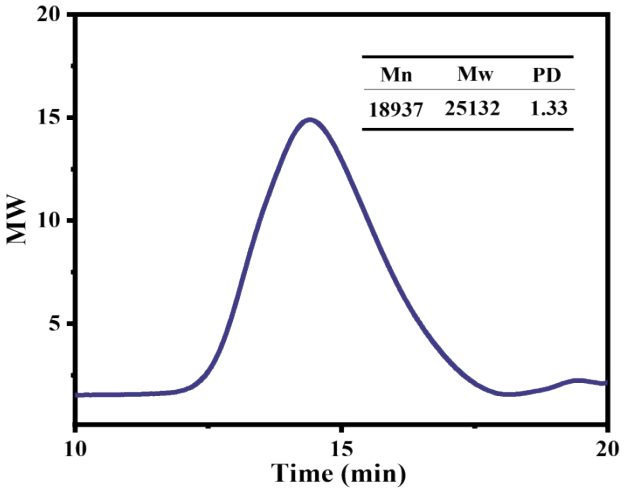

Fig. S9 GPC curve of MPU

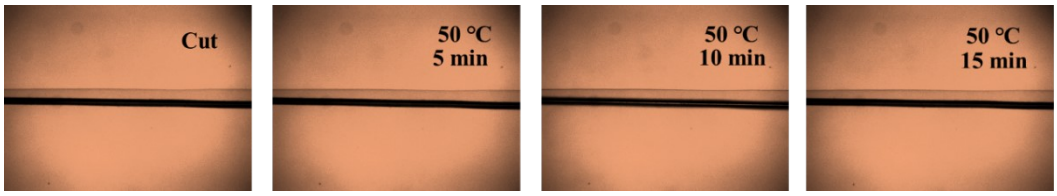

Fig. S10 OM photos of cut control PU at 50°C

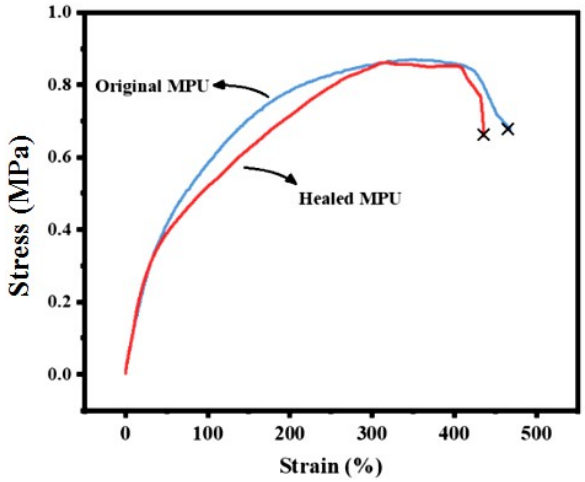

Fig. S11 Stress-strain curves of pristine MPU and healed MPU

Fig. S12 EDS mapping result of PMNs

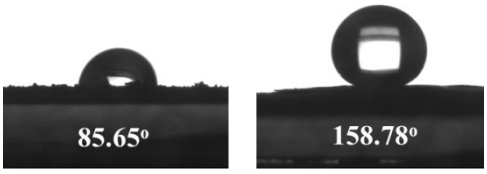

Fig. S13 WCAs of graphene and fluorinate graphene tablets

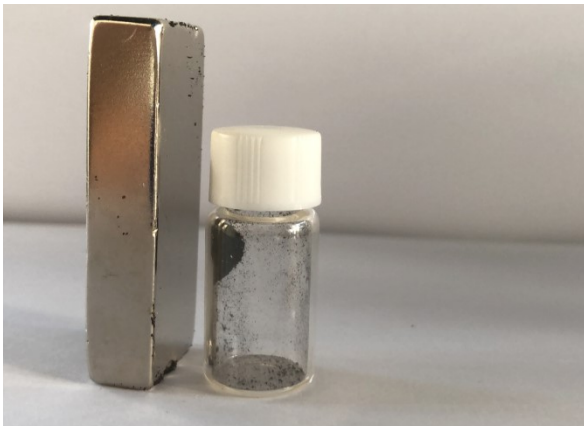

Fig. S14 PMNs-FG attached to the bottle wall by a magnet

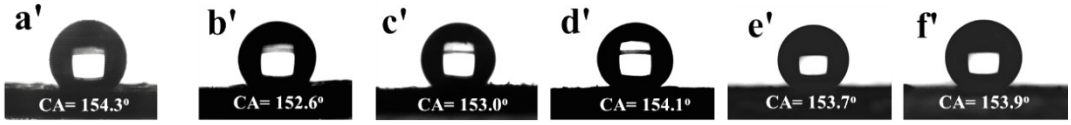

Fig. S15 CAs of different liquids on the surface of PMNs-FG/MPU coating corresponding to Fig. 5a-f

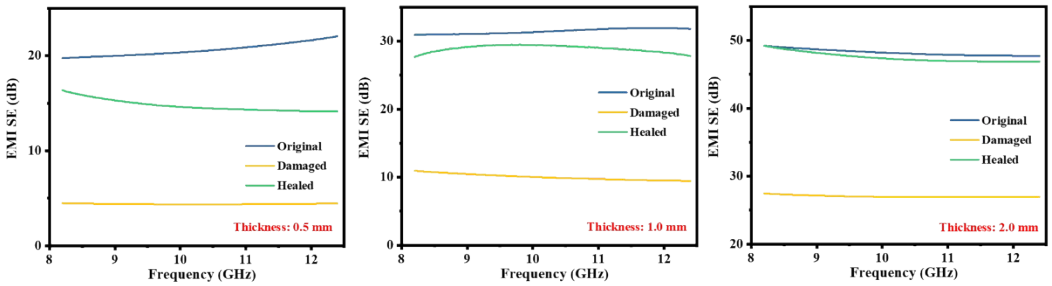

Fig. S16 The EMI SE self-healing efficiency of MNs-FG/MPU films with different thickness

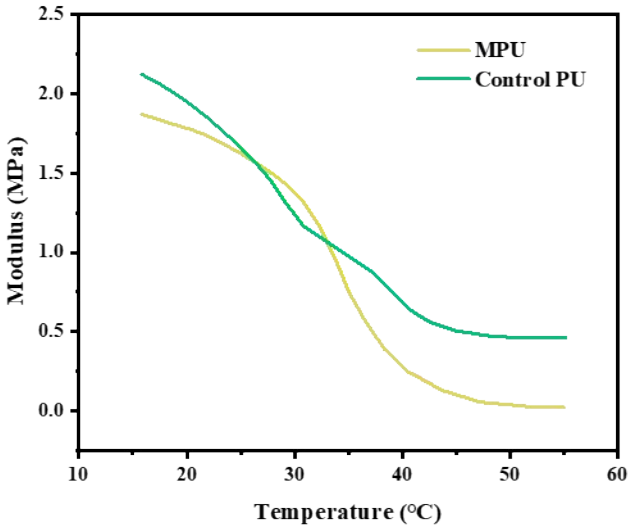

Fig. S17 Dynamic mechanical analysis curves of MPU and the control PU

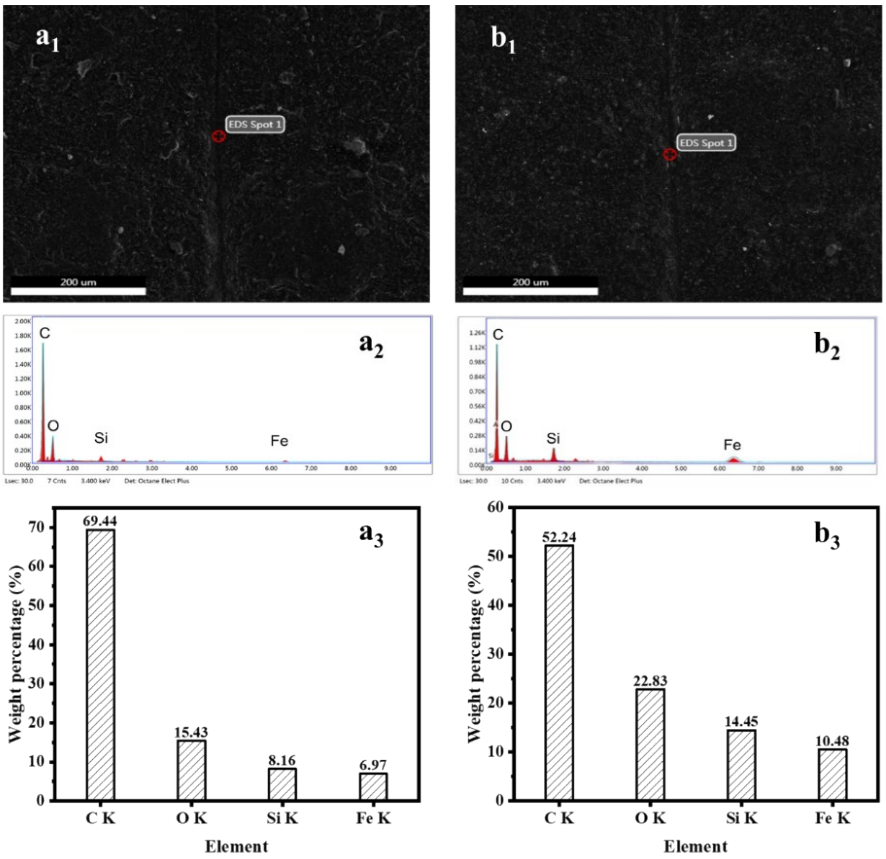

Fig. S18 EDS spot analysis of (a) control PMNs-FG/PU coating (the control coating prepared by the self-healing PU without pyrene groups) and (b) PMNs-FG/MPU coating

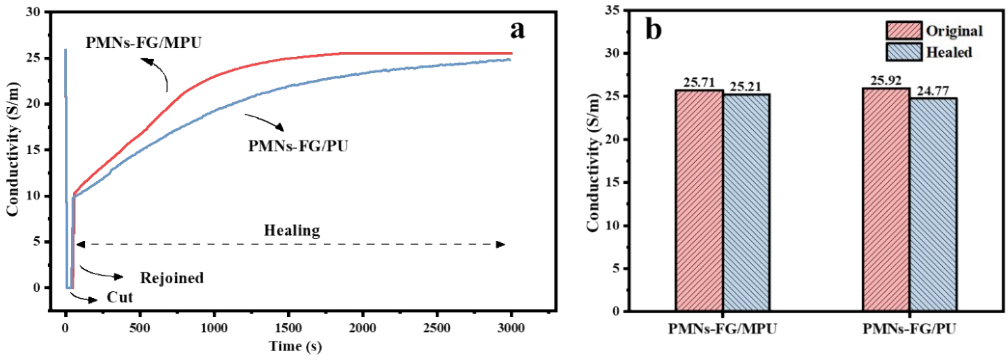

Fig. S19 The conductivity of PMNs-FG/MPU and control PMNs-FG/PU during the healing process

Tab. S1 Comparison of multi-functional composite materials reported in the literature

Composite	EMI SE (dB)	Thickness (mm)	Tensile strength	Self-cleaning (WCA, °)	Self-healing ability	Triggers for healing	Ref.
CNT–MLGEP foam (0.0089 g cm^{-3})	66	3.2	0.043	/	No	/	1
rGO@MoS2@Fe_3O_4	43.6	5	1.06	/	Yes	Heat	2
Silicone-coated M-textile（150 S m^{-1}）	20.5	0.45	/	126	No	/	3
AgNW aerogel/PDMS composite	45	2	~1	~110	No	/	4
CNT/Graphene/WPU	15	0.35	15	95	No	/	5
MXene/HEC/Silicon composite	~74	2	0.22	151.5	No	/	6
MTMS-M/FG	34.6	0.5	/	~138	No	/	7
MXene/PU@MS	20-90	2	/	/	Yes	Force	8
CNT-PHEMA non-woven fabric	10-20	2	7.77	/	Yes	Water Vapor	9
PPyn@POTS Cotton Fabric	25	~0.5	/	153.8	Yes	Microwave	10
STF Label	/	~0.3	0.2	155	Yes	Heat	11
NH_2−MWCNTs/DA-epoxy resin	/	/	22.5	/	Yes	Heat/NIR laser light	12
PMNs-FG/MPU films	~20, ~30, ~50, ~80	0.5, 1.0, 2.0, 3.0	1.5	154.3	Yes	Heat, Solar light, electricity	This work

References

1. Q. Song, F. Ye, X. Yin, W. Li, H. Li, Y. Liu, K. Li, K. Xie, X. Li, Q. Fu, L. Cheng, L. Zhang, B. Wei, *Adv. Mater.,* 2017, **29***,* 1701583.

2. A. V. Menon, B. Choudhury, G. Madras, S. Bose, *Chem. Eng. J.,* 2020, **382**, 122816.

3. Q.-W. Wang, H.-B. Zhang, J. Liu, S. Zhao, X. Xie, L. Liu, R. Yang, N. Koratkar, Z.-Z. Yu, *Adv. Funct. Mater.,* 2019, **29**, 1806819.

4. Z. Zeng, W. Li, N. Wu, S. Zhao, X. Lu, *ACS Appl. Mater. Interfaces,* 2020, **12**, 38584.

5. M. Dai, Y. Zhai, Y. Zhang, *Chem. Eng. J.,* 2021, **421**, 127749.

6. J. Huang, T. Wang, Y. m. Su, Y. Ding, C. Tu, W. Li, *Adv. Mater. Interfaces,* 2021, **8**, 2100186.

7. X. Jia, B. Shen, L. Zhang, W. Zheng, *Compos. B Eng.,* 2020, **198**, 108250.

8. W. Ma, W. Cai, W. Chen, P. Liu, J. Wang, Z. Liu, *Chem. Eng. J.,* 2021, **426**, 130729.

9. L. Chen, K. Guo, S.-L. Zeng, L. Xu, C.-Y. Xing, S. Zhang, B.-J. Li, *Carbon,* 2020, **162**, 445.

10. L. Zou, C. Lan, S. Zhang, X. Zheng, Z. Xu, C. Li, L. Yang, F. Ruan, S. C. Tan, *Nanomicro Lett.,* 2021, **13**, 190.

11. X. Su, H. Li, X. Lai, L. Zheng, Z. Chen, S. Zeng, K. Shen, L. Sun, X. Zeng, *ACS Appl. Mater. Interfaces,* 2020, **12**, 14578.

12. Q. Li, M. Jiang, G. Wu, L. Chen, S. Chen, Y. Cao, Y. Z. Wang, *ACS Appl. Mater. Interfaces,* 2017, **9**, 20797.